

Analysis of the performance properties of coating systems for military applications

Norbert Radek¹ , Marek Michalski^{1,2}, Janusz Kamiński³,
Marcin Szczepaniak⁴, Stanisław Kowalkowski⁵

¹ Faculty of Mechatronics and Mechanical Engineering, Kielce University of Technology, Al. 1000-lecia P. P. 7, 25-314 Kielce, Poland

² Firma Handlowa Barwa Jarosław Czajkowski, ul. Warkocz 3-5, 25-253 Kielce, Poland

³ Faculty of Materials Science and Engineering, Warsaw University of Technology, Wołoska 141, 02-507 Warszawa, Poland

⁴ Military Institute of Engineer Technology, ul. Obornicka 136, 50-961 Wrocław, Poland

⁵ Higher School of Professional Education, Plac Powstańców Śląskich 1/201, 53-329 Wrocław, Poland

* Corresponding author's e-mail: norrad@tu.kielce.pl

ABSTRACT

The article contains an assessment of the physicochemical properties of two-layer masking coatings with the possibility of application in military technology. The fabricated double-layer camouflage coatings have innovative features, in particular, a small thickness in relation to those currently offered by global armaments companies. Masking paint systems were tested for performance properties based on microstructure analysis and measurements of surface roughness, adhesion, hardness, and corrosion and erosion resistance tests. Performance tests were conducted for paint systems manufactured with three options: coating system (SP1), coating system modified with carbon nanotubes (SP2), and coating system modified with glass microspheres (SP3). The microstructure analysis showed that the above-mentioned paint systems are characterized by continuity and homogeneity and are free of pores and microcracks. In addition, the paint masking systems have low roughness parameters, good mechanical properties, and high corrosion resistance. The developed and manufactured two-layer coatings can be successfully applied to armaments and military vehicles.

Keywords: camouflage, coating, microstructure, performance properties, weapons and military vehicles.

INTRODUCTION

Since the appearance of people on Earth, there have been battles between them. They will continue to do so in the present and future as well. Masking is one of the effective methods of achieving an advantage over the opponent, both in offensive and defensive actions [1]. Camouflage, by definition, is a type of security for all combat operations and consists of hiding one's own resources and forces from the enemy's reconnaissance or continuously misleading him about the deployment of his own troops [2]. Masking is a very broad term and, depending on the level of command and scope of tasks, can include three

levels: strategic, operational, or tactical (direct) [3, 4]. In turn, due to the means, forces, or specifications used, concealment, posturing, and disinformation are distinguished [5]. Figure 1 presents the division of camouflage and its types.

Temporary camouflage paint systems are related to direct camouflage, defined as “concealing or changing the appearance of individual or group of objects, devices, equipment, weapons and people using handy camouflage means and materials and standard camouflage means during combat operations” [7]. Among the main tasks of effective camouflage with coatings is correcting the unmasking properties [8], i.e., those that allow distinguishing friendly objects from the terrain

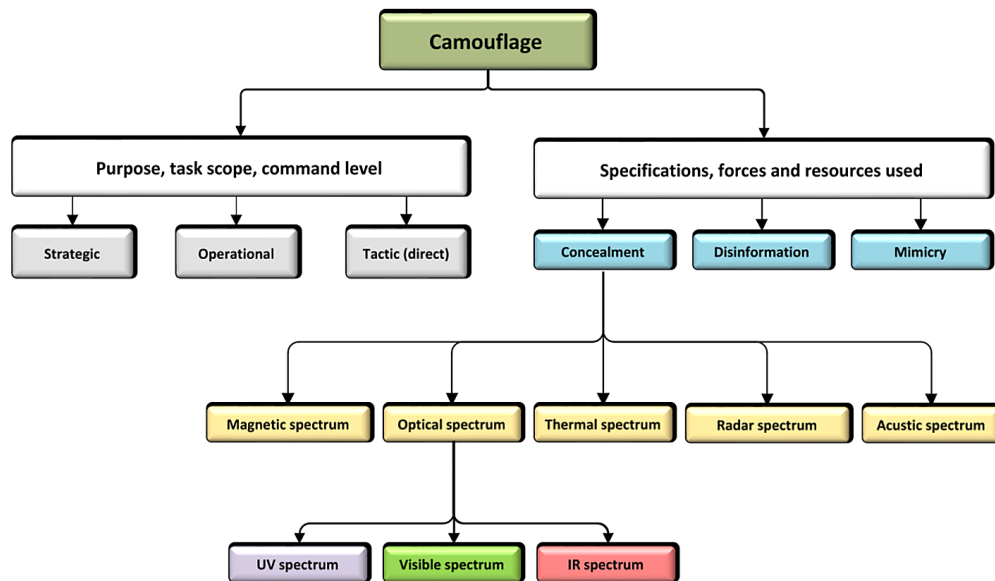


Figure 1. Division of masking and its types [6]

background [9–12] and in the extensive area of electromagnetic radiation: thermal, radiolocation, or optical (UV, visible, IR).

On the modern battlefield, in addition to reconnaissance using the human eye carried out by, for example, reconnaissance units, a number of devices equipped with various sensors are used, including integrated observation heads that may contain, for example, visible light, UV and near-infrared cameras, thermal cameras, multi- and hyperspectral cameras, or radars operating in various bands. As the experience of recent armed conflicts shows (e.g., the war in Ukraine in 2022), the use of consumer UAVs with great success, equipped with sensors used in civilian applications for geodetic or agricultural work, is also becoming common.

At present, there is a rapid development of processes for manufacturing coatings that mainly perform protective and anti-wear functions [13, 14].

It is interesting to note the dynamic progress in the development of paint coatings, which is very fast and multidirectional. Progress in polymer coating technology is due to the following functions: i.e., decorative, protective, and informational. Varnish coating systems account for about 50 percent of paint systems. According to the literature, about 95 percent of all structures made of steel are protected against corrosion by coatings with protective functions, including about 90 percent by paint coatings [15]. It is assumed that the applied coatings perform their operational functions for up to several years.

An important utility property of paint coatings is their low free surface energy, which will make the coatings more resistant to dirt [16, 17].

An important group of coatings are paint coating systems for camouflaging military armaments and vehicles [18, 19]. Lacquer coating systems are the basis of camouflage – hiding military objects in the optical range in both visible VIS light and near-infrared NIR. Effective masking, the main purpose of which is to level the unmasking features, is to not distinguish our own objects from the surrounding terrain to which we can include, for example, texture, color, shape, and gloss [20].

The innovative research attempted to modify green paint, which is commonly used to coat military facilities. The aim of the undertaken activities was to develop formulations and produce camouflage coating systems in the range of spectral characteristics in the range of 350 nm to 1200 nm and color coordinates, as well as provide camouflage in terms of radar recognition.

In the domestic and foreign literature, there is a large gap in scientific work on performance testing of camouflage coating systems for use on military armaments and vehicles.

The work discusses the results of experimental studies of varnish coating systems developed with carbon nanotubes and glass microspheres used in a properly selected coating system. With such a solution, it is possible to achieve camouflage (in terms of optical recognition) in coating systems, which can find application in military technology. The current research refers to

microstructure analysis and measurements of surface roughness, adhesion, hardness, and corrosion and erosion resistance tests.

MATERIALS AND PARAMETERS OF COATING SYSTEM APPLICATION

The specimens with dimensions of $150 \times 100 \times 1$ mm were made of low-carbon steel DC01. The steel samples were first washed with XPA10006 remover to degrease the surfaces. Then, a grinding operation was performed using a rotary machine and P80 grit sandpaper. The final stage of surface preparation was washing the surface with XPA10006 solvent. Masking coating systems were applied in a Blowtherm spray booth and using SATA guns. Masking coating systems were applied by air spray in three options:

- paint system (SP1): primer coating BP450-100/N, masking coating BW400-6031,
- paint system (SP2): primer coating BP450-100/N, masking coating BW400-6031 + carbon nanotube modification (0.02% by weight),
- paint system (SP3): primer coating BP450-100/N, masking coating BW400-6031 + modification with glass microspheres (2.4% mass share).

Masking coating systems were applied according to the scheme shown in Figure 2.

On the basis of our own research, the following parameters for the application of the masking topcoat (green paint) were assumed:

- application technique: pneumatic spray,
- application: two layers,
- surface temperature: 21–23 °C,
- operating pressure: 0.22–0.24 MPa,
- evaporation time between layers: 15 minutes,

- evaporation before baking: 15 minutes,
- annealing temperature: 60 °C,
- annealing time: 60 minutes,
- thickness of dry film: 70–80 μm .

The primer coat was produced according to the paint manufacturer’s technical data. The test was conducted in accordance with the principles of experimental design [21, 22], especially due to the significant contribution of the strongly noising human factor [21, 23]. Statistical analyses included both qualitative [24] and quantitative [25] components.

RESULTS OF EXPERIMENTAL RESEARCH

Morphology

Metallographic examination of the tested samples included grinding and polishing processes to obtain a flat surface. The test samples were cut using a precision cutting machine with a diamond disc Isomet Low Speed from Buehler. The test samples were taken from cross-sections. Abrasive papers (SiC) with grain sizes of 500, 800, 1000, 1200, 2000, 4000, and 5000 were used for grinding. A polishing cloth with a $\frac{1}{4}$ μm silicon suspension was used for polishing. A HITACHI S-3500N scanning electron microscope equipped with a NORAN 986B-1SPS EDS X-ray spectrometer was used to study the morphology of the coating systems.

Figures 3a and 3b show the morphology of carbon nanotubes and glass microspheres. Analysis of the microstructure of carbon nanotubes (Fig. 3a) using electron microscopy showed that they are composed of carbon atoms arranged in one plane and forming a hexagonal structure. Detailed

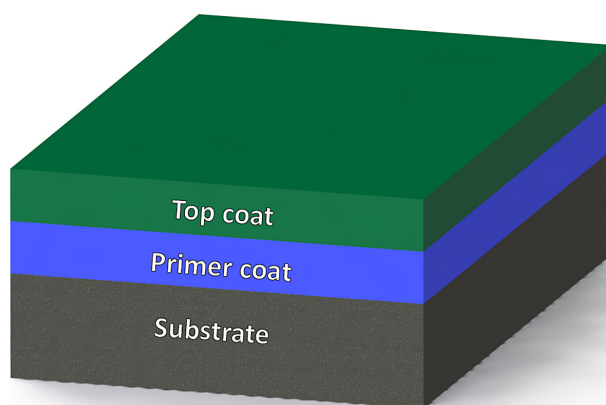


Figure 2. Two-layer coating system

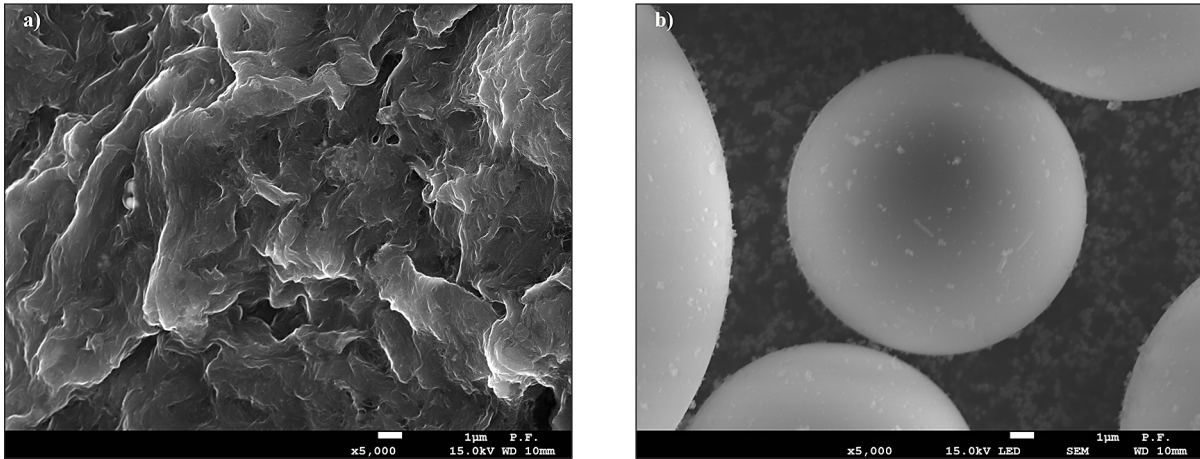


Figure 3. SEM microstructure: a) carbon nanotubes, b) microspheres

SEM studies of microspheres (Fig. 3b) revealed glass, ideal spherical objects with thin walls.

An example of the SEM microstructure of the SP1 coating system is shown in Figure 4. The observations made determined that the minimum thickness of the paint system was about 148 µm. The SP1 coating system had a maximum thickness of about 154 µm. In addition, the primer coating was found to have a thickness in the range of 72–77 µm. Microstructure analysis of the masking system confirmed clear boundaries between the individual layers, the paint system, and the steel substrate (Fig. 4). It was also found that the masking paint system was free of structural defects, i.e., microcracks and pores.

By analyzing the morphology of the remaining SP2 and SP3 coating systems, it was found that the thicknesses of the individual layers included in a given painting system were comparable to the

thicknesses of the layers of the SP1 coating system. The applied masking paint systems for military facilities had thicknesses ranging from about 141 µm to about 157 µm.

Surface roughness measurements

Surface roughness measurements of the coating systems were made using a Talysurf CCI optical instrument. The aforementioned instrument uses the method of coherent correlation interferometry, which gives the possibility of measurement with a z-axis resolution reaching 10 pm. For each paint system, 15 measurements were taken, and the average value was calculated. Roughness profile parameters were calculated as average values from 102 profiles. Masking coating systems for military applications had parameter values of $R_a = 1.8\text{--}2.3\ \mu\text{m}$. Steel samples (after grinding) to

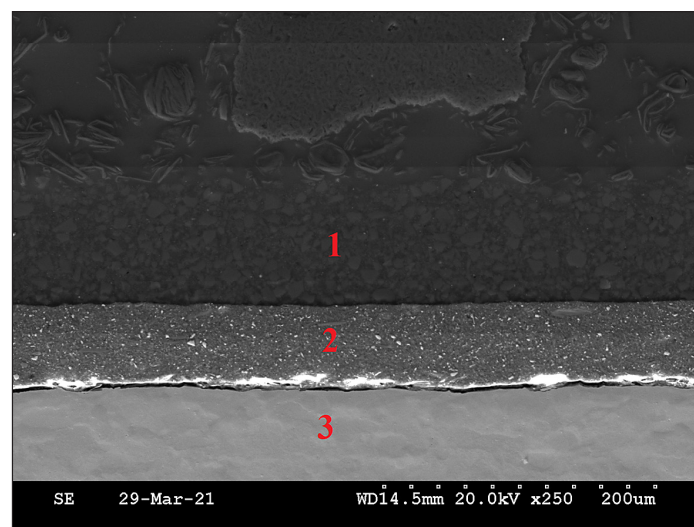


Figure 4. Microstructure of the SP1 masking system: 1– surface layer, 2 – epoxy primer, 3 – steel substrate

which two-layer coatings were applied were characterized by arithmetic mean deviation $Ra = 0.5–0.7 \mu\text{m}$. The averaged parameters of the roughness profile of the studied coating systems are shown in Table 1. The analysis of the results presented (Table 1) shows that the lowest value of the Ra parameter was obtained for the SP2 coating system. The Ra and Rz parameters of the SP3 paint system had the highest values. Figures 5–7 show example surface roughness profiles of the tested paint systems.

Adhesion tests

Measurements of adhesion by scratching were made using a Revetest Xpress Scratch Tester instrument. The test allowed the characterization of

the paint layer/substrate system and the determination of parameters such as friction force and adhesion strength. The characteristics of the scratch tester used are:

- optical observations, friction force, and scratch depth,
- critical load evaluation parameters,
- Rockwell spherical indenter,
- automated microscopic observations.

The measure of adhesion is the value of the critical force, which causes the coating (coating system) to lose adhesion with the substrate.

Two-layer masking coatings SP1, SP2, and SP3 were tested. The parameters of the paint system scratch test were as follows: load growth rate

Table 1. Averaged roughness profile parameters

Parameter	Masking coating system		
	SP1	SP2	SP3
$Rp, \mu\text{m}$	5.496	5.252	7.487
$Rv, \mu\text{m}$	6.766	7.200	5.947
$Rz, \mu\text{m}$	1.262	12.452	13.435
$Rc, \mu\text{m}$	5.092	8.356	6.006
$Rt, \mu\text{m}$	12.262	15.329	13.435
$Ra, \mu\text{m}$	2,219	1.761	2.257
$Rq, \mu\text{m}$	2.716	2.289	2.693
Rsk	-0.826	-0.408	-0.010
Rku	2.660	3.374	2.563
$RSm, \mu\text{m}$	0.100	0.153	0.134
$Rdq, ^\circ$	15.365	15.541	12.986

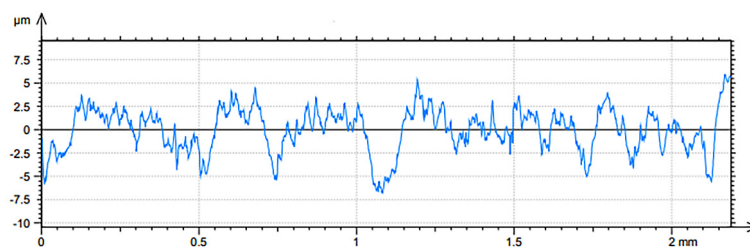


Figure 5. Roughness profile of the SP1 paint system

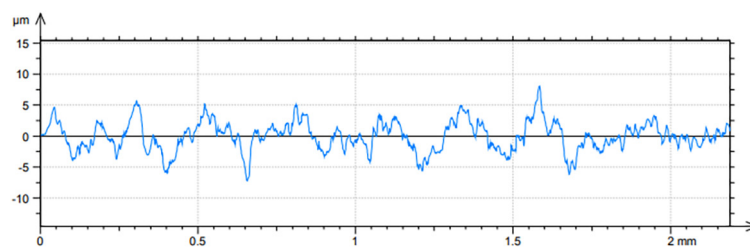


Figure 6. Roughness profile of the SP2 paint system

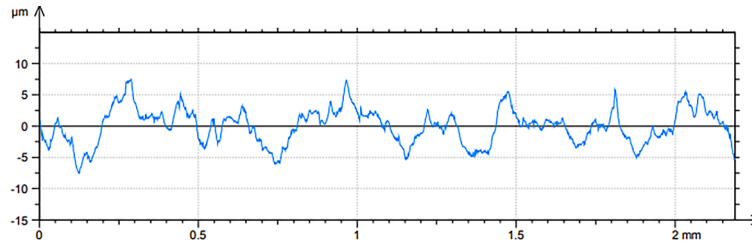


Figure 7. Roughness profile of the SP3 paint system

11 N/min; sample table travel speed 4.49 mm/min; load 50 N; length of scratch 20 mm.

A record of changes in frictional force and microscopic testing (an optical microscope built into an adhesion measuring device) were used to evaluate the value of the critical force. Sample test results are shown in the graph (Figure 8). Meanwhile, Table 2 contains the critical force values from the 5 measurements for a given coating system, as well as their calculated mean values and standard deviation. The obtained results were analyzed by one-way ANOVA. The differentiation of mean values was confirmed (one-way ANOVA, $p = 0.006$) with the assumption of equality of variances (Levene’s test, $p = 0.12$). The mean values of SP1 differ significantly from SP2 and SP3,

while SP2 and SP3 form an indistinguishable homogeneous group (Tukey’s test, SP1-SP2 $p = 0.02$, SP1-SP3 $p = 0.01$, SP2-SP3 $p = 0.90$).

Analyzing the data in Table 2, it was found that the paint systems had good adhesion with the steel substrate. Calculated from three measurements, the average critical force value for each paint system ranged from 41.38 to 46.49 N. It was found that the paint coating systems were characterized by high homogeneity and tightness due to the low dispersion of critical loads.

The highest adhesion to the substrate was demonstrated by the SP3 coating system. The calculated average value of the critical force of the aforementioned paint system was 46.49 N. In contrast, the SP1 coating system had the lowest

Table 2. Adhesion measurement results

Coating system	Critical force, N					Average value and standard deviation, N
	Replication					
	1	2	3	4	5	
SP1	45.15	38.71	40.27	39.36	43.39	41.38±3.36
SP2	44.92	45.39	47.35	44.73	47.05	45.89±1.29
SP3	47.48	46.83	45.16	45.29	47.69	46.49±1.20

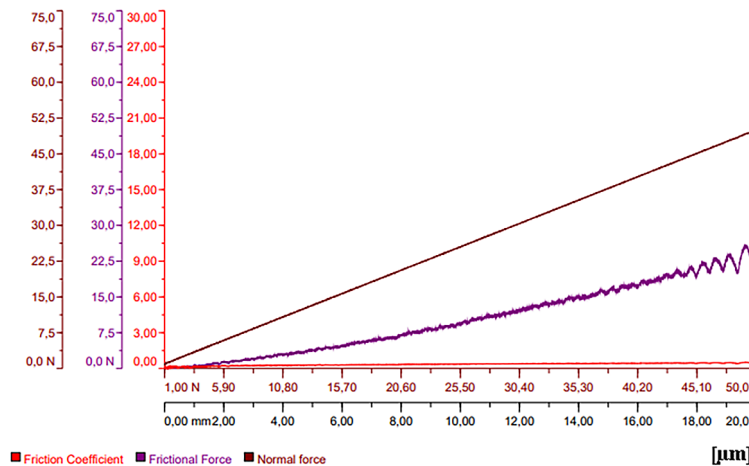


Figure 8. Adhesion measurement record for SP2 coating system

adhesion, with an average critical force value of 41.38 N, 11% lower than that of the SP3 system. For a more accurate determination of the critical forces that cause the loss of adhesion of the coating to the substrate, microscopic methods should be used, which will allow more conclusive results.

There is no information in the world or domestic literature on adhesion testing of masking coating systems using the scratch method. The obtained measurement data will undoubtedly be a valuable source of information for people dealing with the topic of masking coatings used in military technology. The issues related to adhesion measurements using the scratch method are discussed in research works [26].

Adhesion tests of the masking systems carried out showed very similar behavior of the paint coatings and, at the same time, little effect of the thickness of the tested paint systems on the values of critical forces. An example of a Hirox KH-8700 light microscope (LM) image of the topcoat of the SP2 coating system under test after adhesion testing is shown in Figure 9. Hardness measurement by pendulum damping method

The hardness measurement was performed in accordance with PN-EN ISO 1522. In the study, the damping time of the pendulum is measured. The legs of the pendulum are placed on the surface of the sample. The Koenig pendulum was used for the measurements. During the measurement, the number of oscillations during the damping time of the

pendulum was counted from the level of deflection of 6° to 3° from the vertical. A photocell was used to count the oscillations. The number of oscillations was converted to the damping time of the pendulum. In a properly calibrated device using the Koenig pendulum, one oscillation corresponds to 1.4 seconds. Three measurements were made on each sample to average the hardness results obtained according to the thickness of the coating system. The principle of the measurement was to change the friction surface between the coating under test and the pendulum legs, which translates into the damping time of the pendulum. Coatings with lower hardness more easily yield to the weight of the pendulum, whose legs penetrate the coating more deeply, resulting in an increase in friction surface area.

The hardness measurement results using the Koenig pendulum damping method are presented in Table 3. The obtained results were analyzed by one-way ANOVA. The differentiation of mean values was confirmed (one-way ANOVA, $p = 0.006$) with the assumption of equality of variances (Levene's test, $p = 0.15$). The mean values of SP3 differ significantly from SP1 and SP2, while SP1 and SP2 form an indistinguishable homogeneous group (Tukey's test, SP1-SP2 $p = 1.00$, SP1-SP3 $p = 0.01$, SP2-SP3 $p = 0.01$).

The SP3 coating system was characterized by the lowest pendulum damping value (61 s) compared to the SP1 and SP2 painting systems, which had the longest pendulum damping time (70 s).

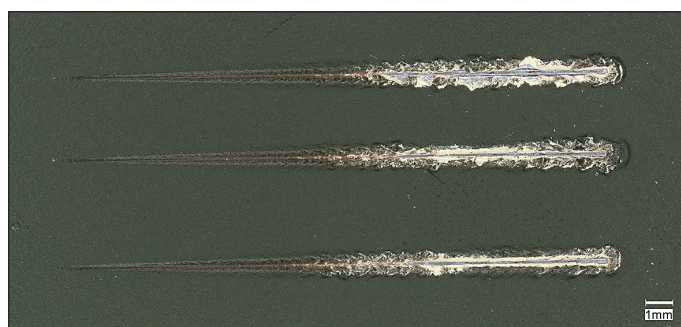


Figure 9. LM image of SP1 coating system after scratch test

Table 3. Hardness measurement results – Koenig pendulum

Coating system	Mean damping time of the Koenig pendulum, s					Average value and standard deviation, N
	Replication					
	1	2	3	4	5	
SP1	73	67	71	67	73	70±3
SP2	69	69	73	68	72	70±2
SP3	54	63	66	54	67	61±6

Tests of resistance to erosion wear

The erosive wear process is a very unfavorable phenomenon that causes the degradation of machine elements in a way that is difficult to predict at the design stage. The process of impact erosion occurs due to the impact of fine particles of abrasive material against the surface of a structural element. The medium in which the particles move can be air or liquid. The intensity of the erosive wear process is influenced by many factors, such as size, hardness, shape of the abrasive material, pressure, speed, temperature of the mixture, and the angle at which the abrasive material hits the eroding element.

Erosion also stimulates gradual abrasion (scratching) of the coating until it is completely removed. Cyclically repeated impacts of hard particles cause fatigue chipping of coating fragments [27]. Destruction of coatings by particles, in the form of scratches and coating defects, intensifies the

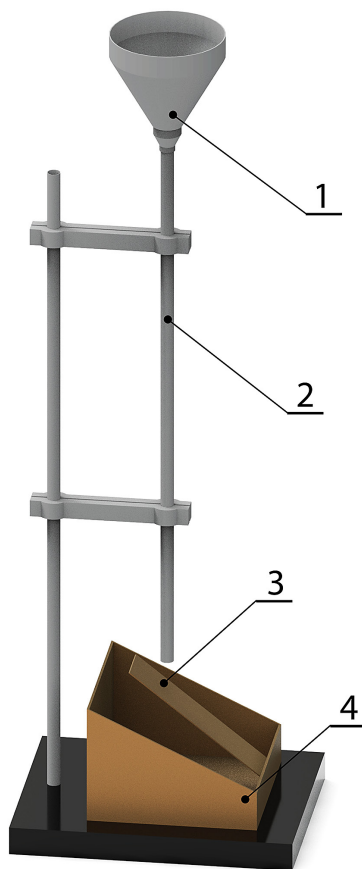


Figure 10. Schematic diagram of the device for testing the erosion resistance of polymer coatings: 1 – hopper, 2 – pipe transporting the abrasive material, 3 – holder for mounting the sample, 4 – container for receiving the abrasive material

corrosive wear of the coating under the impact of aggressive media. The development of subcoating corrosion of the metal substrate results in blistering of the coating and loss of its adhesion [28]. In the study of the erosion wear process of varnish masking systems, the device (Fig. 10) recommended in PN-C-81516:1976 was used. The method consisted of rubbing an elliptical hole in the tested paint coating using a stream of abrasive material. Erosive wear measurements were performed on coating systems SP1, SP2, SP3. Three measurement tests were performed for each paint system, and then the average value of erosive wear was calculated.

The abrasiveness of the tested sample was determined by the ratio of the mass of the abrasive material used to rub the paint coating onto the substrate, expressed in kg, to the average thickness of the tested coating, expressed in μm . During the test, the abrasive material was poured into the hopper, from where it was transported through a pipe set in a vertical position, and by gravity, it fell onto the sample at an angle of 45° . The abrasive material was poured in portions weighing 3.5 kg. The abrasive material used was noble electrocorundum 99A with a grain size of 0.5–0.6 mm. The test was carried out until an elliptical hole in the coating was rubbed through, the larger diameter of which should be 3.6–3.7 mm. After every 10 pourings of the abrasive material, its mass was replenished to the initial 3.5 kg. However, after each hundredth pouring of the abrasive material, the whole was replaced, and the test was continued using 3.5 kg of new corundum. Figure 11 shows a comparison of the erosion resistance of the tested paint systems. The result of erosion resistance was the number of kilograms of erosion material (in this case, electrocorundum) to reduce the thickness of the coating system by one micrometer, expressed by the equation:

$$E = \frac{K}{T} \quad (1)$$

where: E – erosion resistance [$\text{kg}/\mu\text{m}$], K – mass of the abrasive material used for measurement [kg], T – average thickness of the tested coating system [μm].

Paint coating systems (SP1, SP2, SP3) did not differ significantly in terms of erosion resistance, and the results were within the range of 0.77–0.84 $\text{kg}/\mu\text{m}$. The highest erosion resistance was characteristic of the SP1 system (0.84 $\text{kg}/\mu\text{m}$), while the lowest was characteristic of the

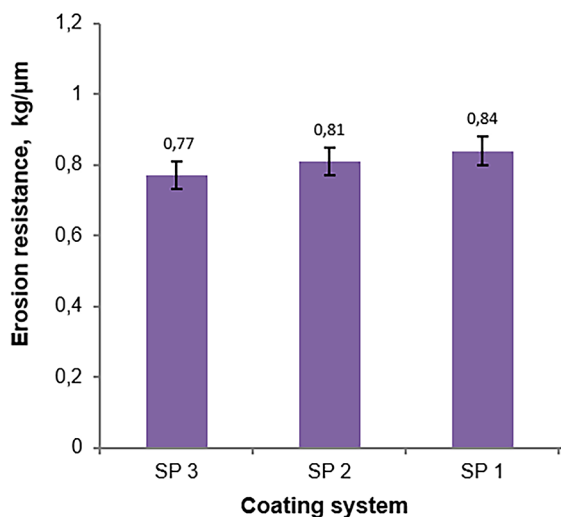


Figure 11. Comparison of erosion resistance of masking coating systems

SP3 system (0.77 kg/μm). The erosion resistance result of the paint systems was most influenced by the applied masking coatings. In practice, the aim is to increase the erosion resistance of the masking coating (while maintaining its good flexibility), which will come into contact with abrasive material (pebbles, sand, etc.) during operation. The destruction of the topcoat layer and then the priming layer will result in a loss of protection against aggressive environmental factors, which may lead to, for example, an accelerated corrosion process. It should be remembered that the intensity of wear of paint coatings increases under the impact of an aggressive environment in the form of brine or acid rain [29].

Corrosion resistance tests

The corrosion resistance tests of paint masking systems were performed using the potentiodynamic method (linear sweep voltammetry – LSV) and the impedance spectroscopy method (electrochemical impedance spectroscopy – EIS) using the AutoLab PGSTAT 100 potentiostat. The electrochemical tests LSV and EIS were performed using a Faraday cage. For the tests, the acid rain solution was used, which was prepared based on the work [30]. Corrosion resistance tests were performed at 21 ± 1 °C.

The tests were performed on samples measuring 80 × 20 × 1 mm on which masking coating systems were applied. Additionally, a blind hole of ø1 mm in diameter and 0.5 mm deep was drilled in the center of each sample. The purpose

of this operation was to penetrate the substrate material in order to speed up corrosion tests.

Potentiodynamic polarization curves were used to designate the corrosion potential (E_{corr}) and corrosion current density (j_{corr}). The extrapolation of Tafel lines is one of the most popular DC techniques for estimating the corrosion rate. The extrapolation of anodic and/or cathodic Tafel lines for charge transfer controlled reaction gives the E_{corr} and j_{corr} , at the corrosion potential. According to the Tafel’s law [31]:

$$E - E_{0,c} = b_c \log (j_c/j_0) \tag{2}$$

is the linear cathodic branch of the polarization curve and:

$$E - E_{0,a} = b_a \log (j_a/j_0) \tag{3}$$

is the linear anodic branch of the polarization curve. In Equations 2 and 3 $E_{0,c}$, $E_{0,a}$, j_0 , b_c , and b_a are constant parameters characterizing polarization curves.

During potentiodynamic testing, cathodic and anodic polarization curves were made by polarizing the samples at a potential change rate of 0.2 mV/s. Samples with an isolated area of 10 mm in diameter were polarized to a potential of 500 mV. The obtained polarization curves of the tested materials are shown in Figure 12.

The shape of the potentiodynamic curve (Fig. 12) indicates uniform corrosion of the tested low-carbon steel in all analyzed cases. The obtained result is caused by the chemical composition of the DC01 steel as well as the acidic pH of the solution (pH4). Both of these factors cause the tested steel to be in an active state, according to the Pourbaix diagram. The cathodic processes, in this case, are the dominant process of oxygen reduction and hydrogen production. The presence of hydrogen gas can cause, in the damage zone, disruptions in the continuity of the tested paint coatings.

Analysis of the graph (Fig. 12) shows that the polarization curves of the masking coating systems are located below the polarization curve of steel. They are characterized by a higher corrosion potential and a significantly lower corrosion current compared to the substrate material. Both of these factors indicate a significant enhancement in the corrosion resistance of varnish systems compared to the starting material. Table 4 summarizes the main electrochemical parameters of the tested materials. The assessment of corrosion resistance of the tested coating systems carried out based on the results of classical electrochemical tests

showed comparable values of corrosion potential of $-0.655\text{ V} \div -0.645\text{ V}$ for the tested coating systems. In comparison, DC01 steel was characterized by a corrosion potential value of -0.680 V . The obtained E_{corr} value indicates when the corrosion processes will start on the tested steel substrate. The lower the potential, the greater the material's tendency to corrosion.

The j_{corr} analysis indicates that the highest resistance of corrosion was possessed by the SP2 coating system, whose corrosion current density was $1.37\ \mu\text{A}/\text{cm}^2$, and that of the substrate material $9.82\ \mu\text{A}/\text{cm}^2$. The above-mentioned paint system increased the corrosion resistance by more than six times compared to the starting material (DC01 steel). The remaining coating systems were also characterized by low corrosion current densities and clearly indicated an increase in corrosion resistance in relation to the steel.

Impedance studies (EIS) were conducted in a three-electrode system in the frequency range of $10^5\text{--}10^{-3}\text{ Hz}$, with a sinusoidal signal amplitude of 20 mV , and an open circuit potential. Impedance spectra were analyzed using the EQUIVCRT Baukampa program. The selection of an electrical

equivalent circuit for the obtained impedance spectra was determined by both the image of corrosion damage and the smallest errors in matching the system elements (determined by the least squares method). The obtained spectra were presented in the form of Nyquist plots (Figures 13–16).

Analyzing the graphs (Figures 13–15), we can observe, in addition to the typical capacitive loop, the presence of an inductive loop. The occurrence of an inductive loop in EIS tests can be caused by several processes, including active and intensive dissolution of the substrate (accelerated anodic processes), adsorption processes of corrosion products, hydrogen release, and pitting corrosion. In the cases analyzed (on the basis of corrosion damage), it can be assumed that there is intensive substrate dilution within the damaged coating. The electrochemical values of the capacitive loop do not depend on the type of coating.

In the case of the substrate material (Fig. 16), due to significant differences in the size of the active surface compared to the analyzed coating systems, the resistance values of DC01 steel are much smaller. On the other hand, the shape of the Nyquist plot is similar to the spectra observed in

Table 4. The main electrochemical parameters

Materials	E_{corr} , mV	j_{corr} , $\mu\text{A}/\text{cm}^2$	$-b_c$, mV/dec	b_a , mV/dec
steel DC01	-680	9.82	573	105
SP1	-650	1.67	1543	154
SP2	-645	1.37	1223	95
SP3	-655	1.41	1851	124

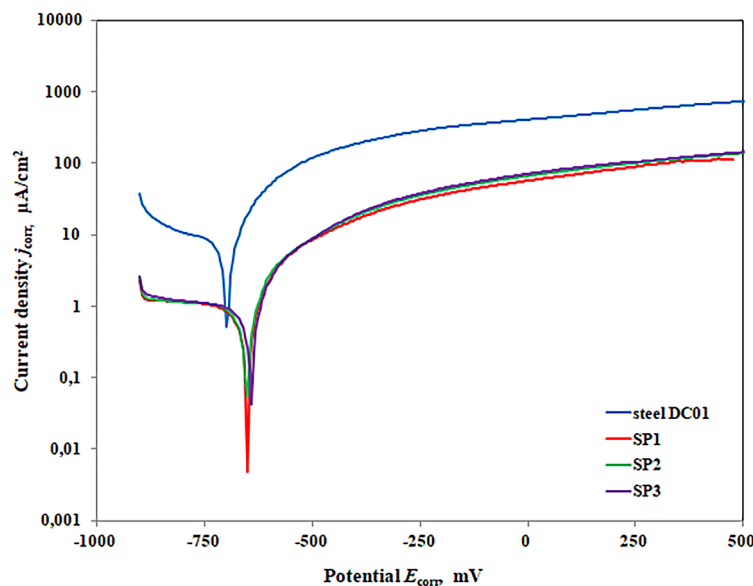


Figure 12. Polarization curves of the tested samples

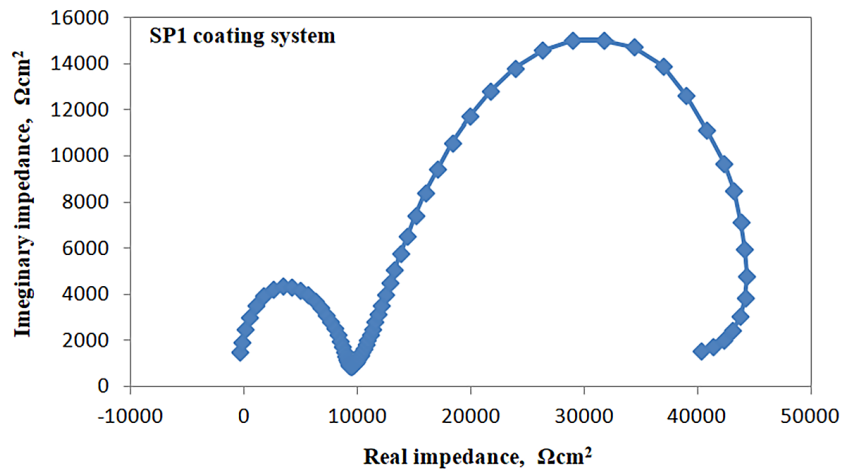


Figure 13. Nyquist impedance spectrum for the SP1 coating system

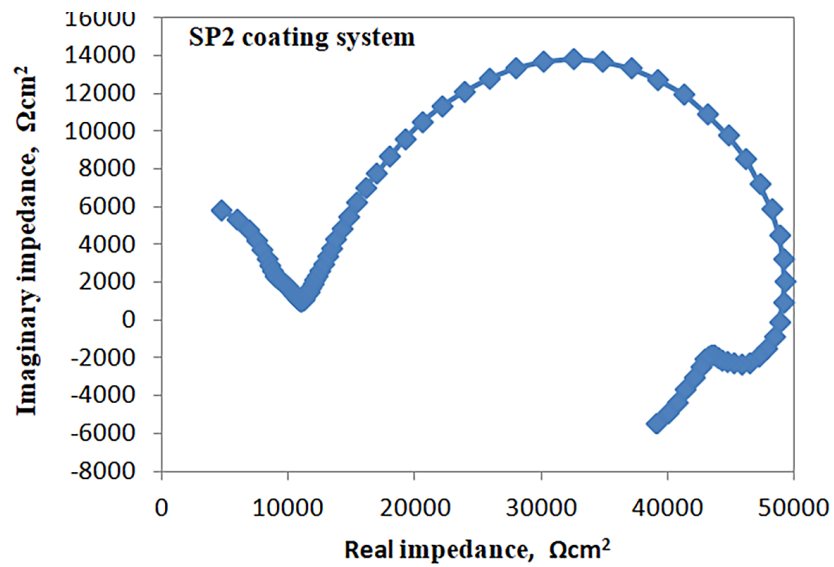


Figure 14. Nyquist impedance spectrum for the SP2 coating system

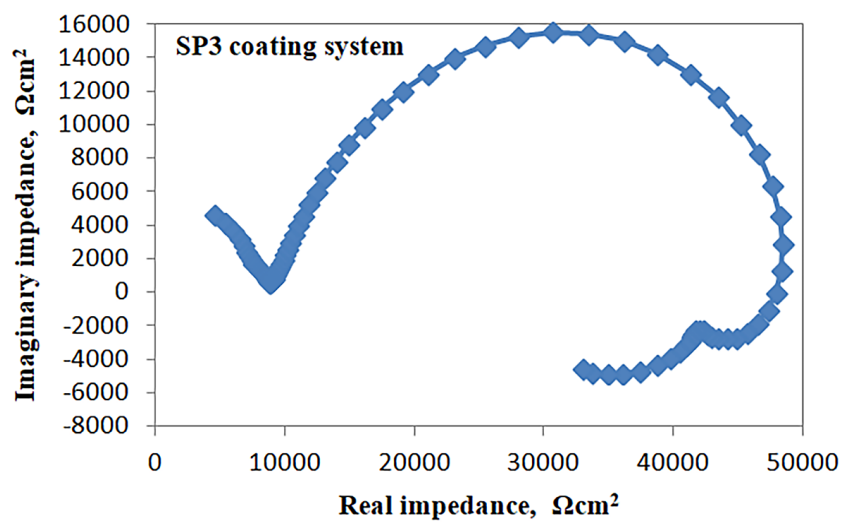


Figure 15. Nyquist impedance spectrum for the SP3 coating system

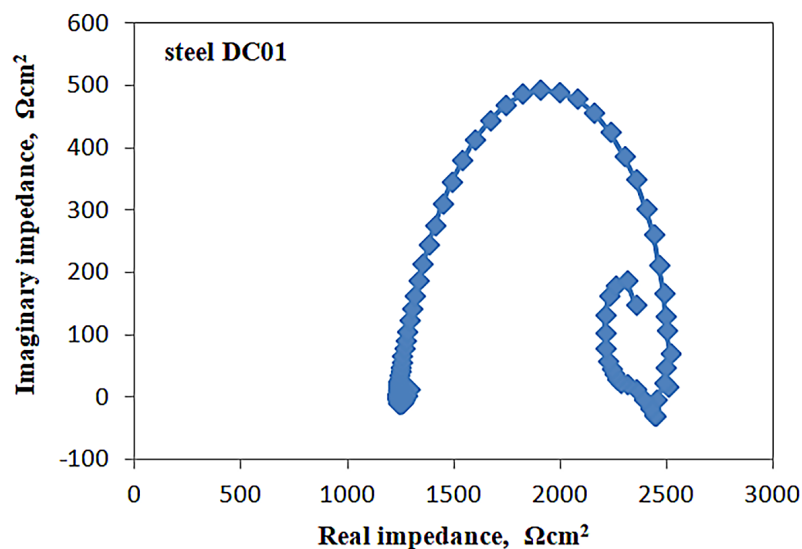


Figure 16. Nyquist impedance spectrum for DC01 steel

the case of two-layer paint coatings. The presence of an induction loop indicates, on the one hand, active dissolution of the steel substrate, while the appearance of an additional capacitive loop (in the low-frequency range) indicates the creation of a layer of solid corrosion products, the presence of which may contribute to the slowing down of corrosion processes.

CONCLUSIONS

As a result of the conducted experimental studies of masking systems, the following conclusions can be drawn:

1. As a result of the microstructure analysis, it was found that the thickness of the coating systems ranged from 141 to 157 μm . It was also observed that the coating systems were free of structural defects, i.e. microcracks and pores.
2. Proper preparation of the substrate material is an important factor affecting the surface roughness of the coating system. The roughness parameters of the two-layer coatings were characterized by higher values compared to the steel substrate (about three times).
3. Analysis of the hardness measurement results using the Koenig pendulum damping method showed that the tested paint systems had similar hardness.
4. The masking systems had good adhesion to the substrate. SP2 two-layer coating had the highest bonding strength.
5. The SP1 and SP2 varnish systems had the

highest erosion resistance, while the SP3 system had the lowest erosion resistance.

6. The paint systems tested were characterized by similar corrosion parameters during exposure. The polarization curves of the paint systems after exposure to acid rain solution were located below the polarization curve of DC01 steel. They were characterized by lower E_{corr} and j_{corr} values relative to the polarization curve of the substrate material.
7. Implementation of innovative two-layer coatings in the Polish Armed Forces will increase the safety of soldiers and military equipment and weapons in the event of combat operations.

REFERENCES

1. Wysocki K., Dąbrowska, I., Idziek, M. Camouflage of troops and facilities based on the experience of selected countries. Warsaw: Faculty of Military, War Studies University; 2020. (in Polish)
2. Cieślak P. Camouflage of troops and facilities. *Przegląd Sił Zbrojnych*. 2017; 2: 8–13. (in Polish)
3. Camouflage of troops and military defense infrastructure, DD/3.20: MON/SG WP; 2010. (in Polish)
4. Przybył W., Mazurczuk, R., Szczepaniak, M., Radek, N., Michalski, M. Virtual methods of testing automatically generated camouflage patterns created using cellular automata. *Materials Research Proceedings*. 2022; 24: 69–77. <https://doi.org/10.21741/9781644902059-11>
5. Derlatka J. Masking - new trends. *Przegląd Sił Zbrojnych*. 2017; 2: 14–17. (in Polish)

6. Plebankiewicz I., Januszko A., Kwak A., Musiał G., Przybył W. Analysis of imagery and spectral data from selected locations in the northern hemisphere and examples of camouflage pattern implementations for these locations. In: Kamyk Z., editor. *Military Engineering - Problems and Perspectives*. Wrocław: Military Institute of Engineer Technology; 2018: 375–384. (in Polish)
7. Bębenek B. Engineering aspects of troop camouflage. *Obronność. Zeszyty Naukowe*. 2017; 1: 5–17. (in Polish)
8. Dojlitko M. Visual message deconstruction theory: military camouflage design tools. Gdańsk: Academy of Fine Arts in Gdańsk; 2015. (in Polish)
9. Newark T. *The Book of Camouflage: The art of Disappearing*. Bloomsbury: Osprey Publishing; 2013.
10. Talas L., Baddeley R.J., Cuthill I.C. Cultural evolution of military camouflage. *Philos TR Soc B*. 2017; 372(1724): art.20160351. <https://doi.org/10.1098/rstb.2016.0351>
11. Toh K.B., Todd P. Camouflage that is spot on! Optimization of spot size in prey-background matching. *Evol Ecol*. 2017; 31(4): 447–461. <https://doi.org/10.1007/s10682-017-9886-3>
12. Yang X., Xu W.-D., Liu J., et al. A small-spot deformation camouflage design algorithm based on background texture matching. *Def Technol*. 2023; 19: 153–162. <https://doi.org/10.1016/j.dt.2021.10.001>
13. Radek N. Determining the Operational Properties of Steel Beaters after Electrospark Deposition. *Eksploatacja Niezawodn.* 2009(4): 10–16.
14. Radek N. Properties of WC-Co coatings with Al₂O₃ addition. *Prod Eng Arch*. 2023; 29(1): 94–100. <https://doi.org/10.30657/pea.2023.29.11>
15. Burakowski T. *Areology - theoretical foundations*. Radom: Scientific Publishing. House of the Institute for Sustainable Technologies - National Research Institute; 2013. (in Polish)
16. Kłonica M. Application of the ozonation process for shaping the energy properties of the surface layer of polymer construction materials. *Journal of Ecological Engineering*. 2022; 23(2): 212–219. <https://doi.org/10.12911/22998993/145265>
17. Kłonica M., Kuczmaszewski J. Modification of Ti6Al4V titanium alloy surface layer in the ozone atmosphere. *Materials*. 2019; 12(13): 2113. <https://doi.org/10.3390/ma12132113>
18. Michalski M., Pisarek U., Radek N., et al. The influence of operational exposure on changes in parameters of effective camouflage of coatings used in military technology. *Adv Sci Technol-Res*. 2023; 17(1): 182–196. <https://doi.org/10.12913/22998624/156940>
19. Radek N., Michalski M., Mazurczuk R., et al. Operational tests of coating systems in military technology applications. *Eksploatacja Niezawodn.* 2023; 25(1): 1–13. <https://doi.org/10.17531/ein.2023.1.12>
20. Przybył W., Januszko A., Radek N., et al. Microwave absorption properties of carbonyl iron-based paint coatings for military applications. *Def Technol*. 2023; 22: 1–9. <https://doi.org/10.1016/j.dt.2022.06.013>
21. Pietraszek J., Goroshko A. The heuristic approach to the selection of experimental design, model and valid pre-processing transformation of DoE outcome. *Adv Mater Res-Switz*. 2014; 874: 145–149. <https://doi.org/10.4028/www.scientific.net/AMR.874.145>
22. Styrylska T., Pietraszek J. Numerical modeling of non-steady-state temperature-fields with supplementary data. *Z Angew Math Mech*. 1992; 72(6): T537–T539.
23. Skrzypczak-Pietraszek E., Pietraszek J. Seasonal changes of flavonoid content in L. (Lamiaceae). *Chem Biodivers*. 2014; 11(4): 562–570. <https://doi.org/10.1002/cbdv.201300148>
24. Szczotok A., Sozanska M. A comparison of grain quantitative evaluation performed with standard method of imaging with light microscopy and EBSD analysis. *Prakt Metallogr-Pr M*. 2009; 46(9): 454–468. <https://doi.org/10.3139/147.110043>
25. Orman L.J., Radek N., Pietraszek J., Szczepaniak M., et al. Analysis of enhanced pool boiling heat transfer on laser-textured surfaces. *Energies*. 2020; 13(11): art.2700. <https://doi.org/10.3390/en13112700>
26. Madej M. The effect of TiN and CrN interlayers on the tribological behavior of DLC coatings. *Wear*. 2014; 317(1–2): 179–187. <https://doi.org/10.1016/j.wear.2014.05.008>
27. Kotnarowska D. Types of polymer coating wear processes. Monograph No. 60. Radom: Radom University of Technology Publishing House; 2003. (in Polish)
28. Kotnarowska D., Wojtyniak, M. Influence of ageing on mechanical properties of epoxy coatings. *Solid State Phenomena*. 2009; 147–149: 825–830.
29. Kotnarowska D. Destruction of polymer coatings under the influence of operating factors. Monograph. Radom: University of Technology and Humanities Publishing House; 2013. (in Polish)
30. Liu F., Song, Y. W., Shan, D. Y., Han, E. H. Corrosion behavior of AZ31 magnesium alloy in simulated acid rain solution. *T Nonferrous Metal Soc*. 2010; 20: S638–S642.
31. Poorqasemi E., Abootalebi O., Peikari M., Haqdaret F. Investigating accuracy of the Tafel extrapolation method in HCl solutions. *Corros Sci*. 2009; 51(5): 1043–1054. <https://doi.org/10.1016/j.corsci.2009.03.001>